Macromolecules **1984**, *17*, 2557–2561

Determination of Short-Chain Branching up to C_6 in Low-Density Polyethylenes by High-Resolution Pyrolysis–Hydrogenation Gas Chromatography

Hajime Ohtani and Shin Tsuge*

Department of Synthetic Chemistry, Faculty of Engineering, Nagoya University, Fro-cho, Chikusa-ku, Nagoya 464, Japan

Takao Usami

Plastics Research Laboratory, Mitsubishi Petrochemical Co., Ltd., Tohocho-1, Yokkaichi, Mie Pref., Japan.

Received January 26, 1984

ABSTRACT: Short-chain branching up to hexyl in low-density polyethylenes (LDPE) has been studied by pyrolysis–hydrogenation fused-silica capillary gas chromatography. The branch content was estimated from the relative peak intensities of the characteristic key isoalkanes in the C_{11} region by comparing the data of reference model ethylene–α-olefin copolymers with known content of methyl, ethyl, butyl, amyl, and hexyl branches, respectively. The results obtained are in fairly good agreement with those found by ^{13}C NMR spectroscopy. In general, the short-chain branches in a given LDPE exist in order of abundance butyl > ethyl > amyl > methyl > hexyl branches, regardless of the total branch content. Further, the presence of pair and/or branched branches is also suggested in addition to isolated branches.

The type and concentration of short-chain branching (SCB) in low-density polyethylenes (LDPE), which vary according to the polymerization conditions, affect many properties of the polymer. Therefore, the characterization of the SCB is required. In recent years, quantitative analyses of the SCB have been primarily performed by ^{13}C NMR spectroscopy.[1]

On the other hand, pyrolysis–hydrogenation gas chromatography (PHGC) methods, which require minimal sample size and a simple operating procedure, have also been utilized for the study of the SCB. In earlier work, Michailov et al.[2] identified some of the isoalkane peaks on the hydrogenated pyrograms of LDPE's and pointed out that ethyl and butyl branches predominate. Seeger and Barall,[3] using ethylene–1-butene and ethylene–1-hexane copolymers as standards, detected about 20 ethyl and 10 *n*-butyl branches per 1000 carbons from the high yields of 3- and 5-methylalkanes. The resolution of the pyrograms, however, was insufficient because of the use of packed columns. Ahlstrom and Liebman[4] demonstrated the presence of ethyl and butyl branches from increases in the size of the 3-methylalkanes and *n*-butane peaks, respectively, although 5-methylalkanes were not resolved.

Later, Mlejnek,[5] employing a more effective open tubular column and Curie-point pyrolyzer, obtained high-resolution pyrograms of PE's. On the basis of the relative peak area of isoalkanes, he concluded that the presence of methyl, ethyl, and butyl groups was equally probable in LDPE's. In our recent work,[6-8] glass capillary PHGC was applied to the quantitative analysis of the SCB. Relating the relative peak intensities of characteristic isoalkanes for LDPE's to those of reference model copolymers, we determined methyl, ethyl, and butyl branch contents in LDPE's. Liebman et al.[9] reported a comparable study on the SCB in PE's by fused-silica capillary PHGC and ^{13}C NMR spectroscopy. In order to extend the interpretative capabilities of PHGC, a computer simulation method was applied to reproduce the fragmentation pattern of the pyrogram of LDPE's using the data of known references. They[9] suggested that PHGC can estimate contents of SCB as low as one branch per 10 000 CH_2. Recently, Haney et al.[10] proposed a new PHGC method at relatively low pyrolysis temperature (360 °C). By this method, enhanced yields of the products pertaining to the branch points were observed on the resulting pyrograms of PE's. The observed excess amount of 3-methylpentane from PE's was qualitatively attributed to the existence of Willbourn-type branches such as 2-ethylhexyl (branched branch) and 1,3-paired ethyl (pair branch).

However, the existence of amyl branches and branches longer than hexyl, which has been confirmed by ^{13}C NMR spectroscopy,[11-15] has not been clearly characterized by PHGC mainly because of the lack of well-defined model polymers and of insufficient resolution for the associated isoalkanes on the pyrograms. In this work, PHGC methods for determining the SCB in LDPE's are extended up to hexyl branches using a high-resolution fused-silica capillary column and well-characterized model copolymers. Branch content thus estimated is compared with that obtained by ^{13}C NMR spectroscopy. In addition, the possible existence of pair and branched branches is also discussed on the basis of theoretical and observed yields for 5-ethylnonane, which is characteristic of the ethyl branch.

Table I
Type and Content of Branches in the Reference Ethylene–α-Olefin Copolymers

sample	α-olefin comonomer	branch type	branch content[a]
EP	propylene	methyl	20
EB	1-butene	ethyl	24
EHX	1-hexene	butyl	18
EHP	1-heptene	amyl	12
EO	1-octene	hexyl	20

[a] Branch content/1000 C determined by IR spectroscopy.

Experimental Section

Samples. The four representative commercial high-pressure LDPE samples studied are identical with those in ref 15. The five kinds of ethylene–α-olefin copolymers used as references are listed in Table I. The branch content was determined by IR spectroscopy using the corrected absorbance at 7.25 μm.[16] The conversion coefficients from the absorbance to the degree of branching were established from the relationship between the IR absorption intensity and the radioactivity for each type of copolymer of ethylene and α-olefin labeled with ^{14}C.[17,18] Both the reference copolymers and their IR data were kindly supplied by Sumitomo Chemical Industry Co., Ltd., through the courtesy of M. Kakugo.

Conditions for PGC. The pyrolysis-hydrogenation capillary gas chromatographic system utilized in this work is basically the same as that described previously.[8] A vertical microfurnace-type

0024-9297/84/2217-2557$01.50/0

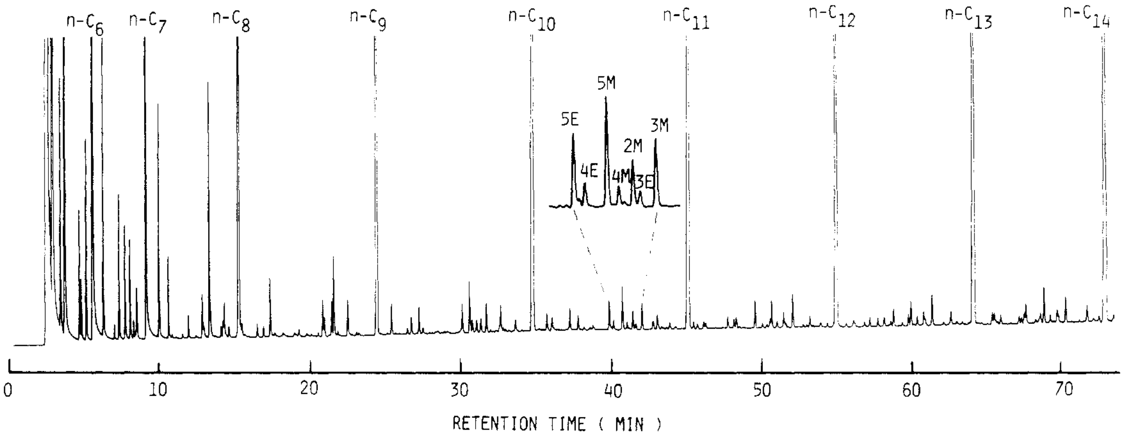

Figure 1. A high-resolution pyrogram of LDPE-B at 650 °C: 2M, 2-methyldecane; 3M, 3-methyldecane; 4M, 4-methyldecane; 5M, 5-methyldecane; 3E, 3-ethylnonane; 4E, 4-ethylnonane; 5E, 5-ethylnonane.

Table II
Possible Fragmentation Products of C_{11} from the Site of Branching in PE

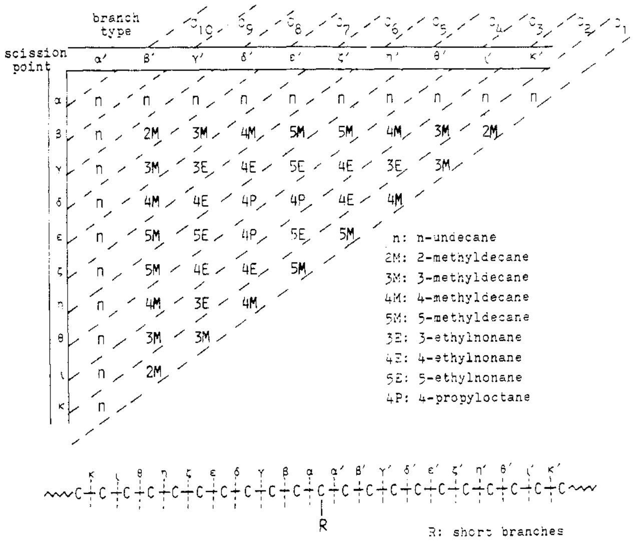

scission point	α′	β′	γ′	δ′	ε′	ζ′	η′	θ′	ι′	κ′
α	n	n	n	n	n	n	n	n	n	n
β	n	2M	3M	4M	5M	5M	4M	3M	2M	
γ	n	3M	3E	4E	5E	4E	3E	3M		
δ	n	4M	4E	4P	4P	4E	4M			
ε	n	5M	5E	4P	5E	5M				
ζ	n	5M	4E	4E	5M					
η	n	4M	3E	4M						
θ	n	3M	3M							
ι	n	2M								
κ	n									

n: n-undecane
2M: 2-methyldecane
3M: 3-methyldecane
4M: 4-methyldecane
5M: 5-methyldecane
3E: 3-ethylnonane
4E: 4-ethylnonane
5E: 5-ethylnonane
4P: 4-propyloctane

R: short branches

pyrolyzer (Yanagimoto GP-1018) was directly attached to a gas chromatograph (Shimadzu 7AG) with a fused-silica capillary column supplied by Hewlett-Packard (0.32-mm o.d. × 0.2-mm i.d. × 50 m long) which was wall-coated with OV-1 and immobilized by chemical cross-linking. A small piece of precut column (3-mm i.d. × 5-cm long) containing 5 wt % of OV-101 packing (80/100 mesh Diasolid-H) and a hydrogenation catalyst column (3-mm i.d. × 10-cm long) containing 5 wt % of Pt packing (80/100 mesh Diasolid-H) was inserted in series between the pyrolyzer and a splitter with a splitting ratio of 1:40. Both the precut and the catalyst columns were maintained at 200 °C. The precut column was used to protect the catalyst and the separation column from tarry and/or less volatile degradation products. The column temperature was held initially at 30 °C for 2 min and programmed at a rate of 1.5 °C/min up to 280 °C. A sample size of about 500 μg was pyrolyzed at 650 °C under a flow of hydrogen carrier gas (50 mL/min).

Results and Discussion

Figure 1 shows a typical high-resolution hydrogenated-product pyrogram obtained for a LDPE by use of the fused-silica capillary column. As compared with the previous pyrograms for LDPE's,[8] drastic improvement in resolution was attained for the isoalkanes which are closely related to the SCB. Although the peak resolution between 2-methyldecane (2M) and 3-ethylnonane (3E) in the C_{11} region was not sufficient with an ordinary glass capillary column, almost complete separation was attained by using the fused-silica column. Thus, the determination of the SCB was carried out on the basis of characteristic peak intensities in the C_{11} region according to the same approach reported previously.[8]

Table II summarizes the possible fragmentation products of C_{11} formed from the short-branch structures in the polymer chain provided that any side-chain cleavages do not occur. Each compartment divided by oblique dotted lines depicts the fragments corresponding to each type of branching from C_1 to C_{10}. In the following discussion, however, branches up to hexyl were taken into consideration except for propyl branches, whose existence in LDPE's, if any, is known to be negligibly small.

Figure 2 represents the expanded portions of the pyrograms for reference model copolymers along with a LDPE between the n-C_{10} and n-C_{11} region. The most intense isoalkane peak was chosen as the key peak for each type of branch except for amyl branches. The most intense peak for amyl was 5M (5-methyldecane), which was also the most intense for butyl, so that the second most intense peak, 4E (4-ethylnonane) was allocated for the key peak for amyl instead of 5M. Thus, the correlation factors (f) for the content of branches defined previously[8] were first calculated from the corresponding data for the model copolymers with known branch content

$$I(\text{key})_{\text{obsd}}f = \text{branch number}/1000\ \text{C} \qquad (1)$$

where $I(\text{key})_{\text{obsd}}$ was the relative value when the observed

Table III
Relative Peak Intensities of Isoalkanes to Key Peak and Observed Correlation Factors for Reference Copolymer

reference polymer	branch content per 1000 C	I_{obsd}[a]	f[b]	relative peak intensities of isoalkanes to key peak[c]							
				2M	3M	5M	4E	4M	3E	5E	4P
EP	20 methyl	77.3 (2M)	260	1.00	0.46	0.44		0.38			
EB	24 ethyl	55.3 (3M)	430	0.10	1.00	0.093	0.33	0.061	0.36	0.16	0.05
EHX	18 butyl	43.5 (5M)	410	0.24	0.17	1.00	0.035	0.095	0.01	0.33	0.2
EHP	12 amyl	20.5 (4E)	590	0.31	0.30	2.52	1.00	0.18	0.031	0.070	
EO	20 hexyl	51.4 (4M)	390	0.21	0.15	0.15	0.032	1.00	0.20	0.025	

[a] Key peak intensities relative to peak intensities of $I(n\text{-}C_{11})_{\text{obsd}} = 1000$. [b] Calculated correlation factor defined by eq 1. [c] The underlined values are for key peaks.

Table IV
Observed and Effective Intensities of Key Peaks

	relative intensity of key peaks[a]				
sample	I(2M)	I(3M)	I(5M)	I(4E)	I(4M)
LDPE-A	5.0	11.4	20.2	3.9	0.5
	(12.5)	(18.5)	(33.6)	(8.6)	(5.8)
LDPE-B	5.8	16.7	27.3	3.7	0.8
	(15.2)	(25.3)	(40.9)	(10.3)	(7.3)
LDPE-C	5.0	11.2	21.0	3.2	1.0
	(12.3)	(18.0)	(32.3)	(7.6)	(6.1)
LDPE-D	3.8	4.9	11.0	1.0	0.8
	(7.4)	(8.9)	(15.7)	(3.0)	(3.7)

[a] Values relative to $I(n\text{-C}_{11})_{\text{obsd}} = 1000$. Effective intensities are given first, and observed intensities are given below in parentheses.

peak intensity of n-C$_{11}$ was regarded as $1000(I(n\text{-C}_{11})_{\text{obsd}} = 1000)$.

Table III summarizes the observed $I(\text{key})_{\text{obsd}}$ and the calculated f values together with the relative peak intensities of the isoalkanes to the corresponding key peaks. The data of the relative peak intensities of the isoalkanes in Table III, however, suggest that each key peak is not completely independent of others. For example, 3M used as the key peak for ethyl branch is also formed from the other branching structures such as methyl, butyl, amyl, and hexyl according to the side-chain cleavages which are not taken into consideration in the discussion of Table II but actually are involved in the thermal degradation of the branched polymers to some extent, in addition to the possible fragmentation scheme shown in Table II. Therefore, considering the mutual contributions of the other key peaks observed for the five model copolymers shown in Table III, the effective peak intensity, I_{eff} for each key peak proposed in the previous paper[8] can be calculated by solving the following simultaneous equations:

$$\left.\begin{aligned}
&I(2\text{M})_{\text{eff}} + 0.10I(3\text{M})_{\text{eff}} + 0.24I(5\text{M})_{\text{eff}} + \\
&\qquad 0.31I(4\text{E})_{\text{eff}} + 0.21I(4\text{M})_{\text{eff}} = I(2\text{M})_{\text{obsd}} \\
&0.46I(2\text{M})_{\text{eff}} + I(3\text{M})_{\text{eff}} + 0.17I(5\text{M})_{\text{eff}} + \\
&\qquad 0.30I(4\text{E})_{\text{eff}} + 0.15I(4\text{M})_{\text{eff}} = I(3\text{M})_{\text{obsd}} \\
&0.44I(2\text{M})_{\text{eff}} + 0.093I(3\text{M})_{\text{eff}} + I(5\text{M})_{\text{eff}} + \\
&\qquad 2.52I(4\text{E})_{\text{eff}} + 0.15I(4\text{M})_{\text{eff}} = I(5\text{M})_{\text{obsd}} \\
&0.33I(3\text{M})_{\text{eff}} + 0.035I(5\text{M})_{\text{eff}} + \\
&\qquad I(4\text{E})_{\text{eff}} + 0.032I(4\text{M})_{\text{eff}} = I(4\text{E})_{\text{obsd}} \\
&0.38I(2\text{M})_{\text{eff}} + 0.061I(3\text{M})_{\text{eff}} + 0.095I(5\text{M})_{\text{eff}} + \\
&\qquad 0.18I(4\text{E})_{\text{eff}} + I(4\text{M})_{\text{eff}} = I(4\text{M})_{\text{obsd}}
\end{aligned}\right\} \quad (2)$$

where $I(2\text{M})_{\text{obsd}}$ and $I(3\text{M})_{\text{obsd}}$ are the observed relative peak intensities of the corresponding isoalkanes on the pyrogram of a given LDPE regarding the peak intensity of n-C$_{11}$ alkane (undecane) as $1000(I(n\text{-C}_{11})_{\text{obsd}} = 1000)$. Thus calculated I_{eff}'s for the four LDPE's are listed in

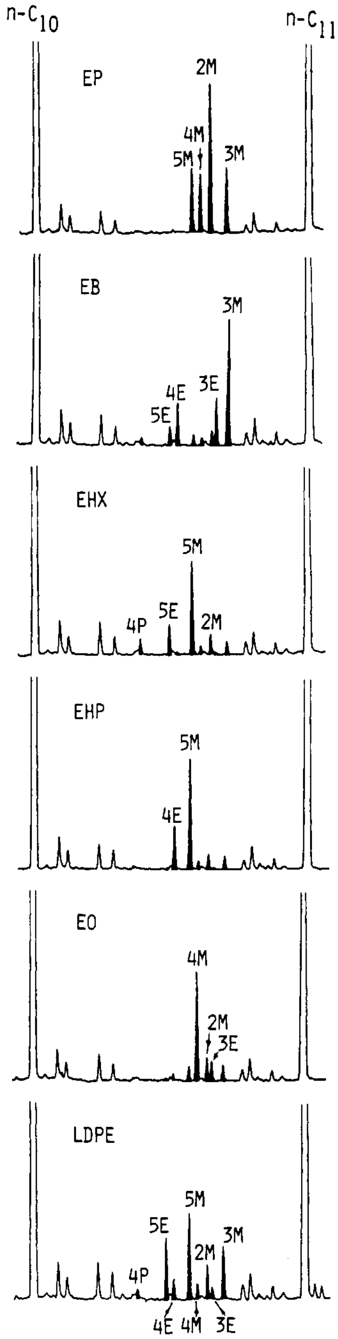

Figure 2. Expanded pyrograms of reference copolymers and LDPE-B in the C$_{11}$ region. 2M, 3M, 4M, 5M, 3E, 4E, and 5E are the same as in Figure 1, and 4P is 4-propyloctane.

Table V
Estimated SCB Content in LDPE's by PHGC and by ^{13}C NMR Spectroscopy

	estimated SCB content/1000 C[a]						
sample	methyl	ethyl	butyl	amyl	hexyl	longer[b]	total[c]
LDPE-A	1.3	4.9	8.3	2.3	0.2		17.0
	(0.4)	(6.4)	(7.4)	(2.6)		(2.8)	(19.9)
LDPE-B	1.5	7.2	11.2	2.2	0.3		22.4
	(0.5)	(7.2)	(8.5)	(2.7)		(3.5)	(24.9)
LDPE-C	1.3	4.8	8.6	1.9	0.4		17.0
	(0.5)	(5.4)	(6.4)	(2.2)		(2.4)	(17.3)
LDPE-D	1.0	2.1	4.5	0.6	0.3		8.5
	(0.1)	(2.3)	(2.4)	(0.7)		(1.0)	(6.7)

[a] Estimated SCB content by PHGC are given first, and estimated SCB content by ^{13}C NMR spectroscopy are given in parentheses. [b] The longer chain branches are not taken into consideration in the case of PHGC. [c] Content by NMR involves also propyl branch content between 0.2 and 0.5.

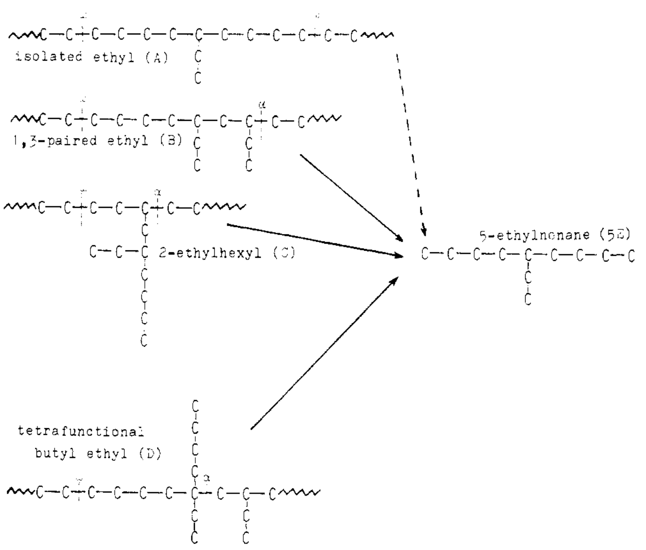

Figure 3. Typical fragmentation of the most probable sites for (A) isolated, (B) 1,3-paired, (C) 2-ethylhexyl, and (D) tetrafunctional butyl ethyl branches in PE to yield 5-ethylnonane (5E).

Table IV along with the observed values, I_{obsd}'s. Subsequently, the SCB content in the LDPE's is calculated by multiplying the I_{eff} by the corresponding correction factor, f, in Table III according to basically the same relation as in eq 1.

Table V summarizes the SCB content obtained by this method for the four LDPE's along with that found by ^{13}C NMR spectroscopy.[15] As a whole, the estimated individual short-branch content and the total values are in fairly good agreement with those obtained by ^{13}C NMR spectroscopy. Generally, the short-chain branches in LDPE's exist in greater abundance in the order of butyl > ethyl > amyl > methyl > hexyl branches regardless of the total branch content. The hexyl branches in LDPE's, so far roughly regarded as negligible by ^{13}C NMR spectroscopy,[12,15] were quantitatively confirmed by this method. When further detailed observations are made, certain common tendencies are observed among the differences in the SCB content for methyl and butyl branching. PHGC always gave a somewhat larger methyl and butyl content than ^{13}C NMR spectroscopy. These differences might be explained by the following discussion.

Since the branches in the reference copolymers can be regarded as isolated from each other, the determination was carried out on the assumption that the branches in LDPE's were randomly distributed. On the other hand, based on the mechanism of formation of the SCB, it has been speculated that the branches in LDPE's are not always isolated from each other. In particular, the expanded back-biting mechanism[19-21] predicted the formation of various complex structures in the polymer chain such as 1,3-paired ethyl (B), 2-ethylhexyl (C) and tetrafunctional butyl ethyl (D) rather than isolated ethyl (A) (Figure 3). Such a multiplicity of the ethyl branch structures has been also reported by ^{13}C NMR studies.[14,15,22-25]

Table VI
Observed and Calculated Peak Intensities of 5-Ethylnonane (5E)

sample	I_{obsd}(5E)[a]	I_{calcd}(5E)[b]
LDPE-A	18.3	8.8
LDPE-B	26.7	11.9
LDPE-C	18.6	8.8
LDPE-D	6.8	4.5

[a] Observed intensities relative to $I(n\text{-C}_{11})_{\mathrm{obsd}}$ = 1000. [b] Values calculated from the obtained branch content in Table V and relative peak intensities of 5E in Table III.

According to the empirical observations of thermal degradation of branched polyolefins,[3,6,8,10] the carbon–carbon bonds α and β to the branch point cleave with higher probabilities than the farther bonds (γ, δ, ϵ, etc.). Thus, the fact that the methyl branch content observed by this method is always slightly higher than those found by ^{13}C NMR spectroscopy could be attributed partly to the existence of the 2-ethylhexyl structure (C) and of the branches longer than hexyl. The former branched branch structure is most liable to be cleaved at the α position to form a secondary methyl branch structure and a n-alkane (C_7) as follows:

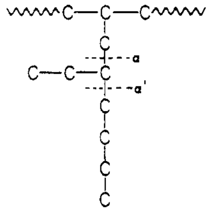

This is one probable reason for the observed higher methyl branch content. If the next most probable cleavage occurs at the α' position, the secondary butyl branch structure is formed which contributes the higher values for butyl branches by this method. On the other hand, the most probable characteristic isoalkane of C_{11} pertaining to the longer branch structures (>C_6) is 2-methyldecane (2M), formed mostly through β, β', and ω cleavages as follows:

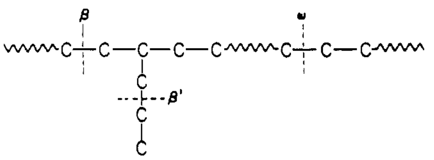

This is another possible source for the slightly higher methyl branch content found by this method.

The complex branch structures predicted by the expanded back-biting mechanisms such as (B), (C), and (D) shown in Figure 3 would yield predominantly 5-ethylnonane (5E) in the C_{11} region through the most probable α and ω cleavages. On the other hand, 5E has to be formed from the isolated ethyl structure (A) only through random scission at ω and ω' rather than preferentially. Hereupon, theoretical 5E peak intensities supposing random distribution of the SCB along the polymer chain can be calculated from the estimated branch content by this method (Table V) considering the fragmentation pattern factors for the model copolymers (Table III) where the associated branch structures can be regarded as highly isolated. Thus calculated data of $I(5\mathrm{E})_{\mathrm{calcd}}$ are compared with those observed, $I(5\mathrm{E})_{\mathrm{obsd}}$, in Table VI for the four LDPE's. The fact that the $I(5\mathrm{E})_{\mathrm{obsd}}$'s always take fairly higher values than the $I(5\mathrm{E})_{\mathrm{calcd}}$'s would suggest the significant contribution of such complex branch structures as (B), (C), and (D) in the polymer chain of the LDPE's.

In this paper, we have described that the PHGC method by use of a high-resolution fused-silica capillary column is a very effective tool for determination of the SCB in LDPE's with short analysis time and minimal amounts of sample (0.5 mg). Moreover, the existence of pair and/or branched branches in the LDPE's was also suggested. Further improvements could be attained by incorporating (a) a higher resolution column to enable detection of even the minor isoalkane peaks on the pyrogram, (b) additional well-characterized model copolymers, especially for the expected complex branching structures such as that in ethylene–4-ethyl-1-octene copolymer, etc., and (c) the computer simulation of the fragmentation patterns.

Acknowledgment. We are indebted to M. Kakugo, Sumitomo Chemical Industry Co., Ltd., for providing a series of well-characterized ethylene–α-olefin copolymers and for his helpful discussion.

References and Notes

(1) Bovey, F. A.; Schilling, F. C.; Starnes, W. H., Jr. *Polym. Prepr., Am. Chem. Soc., Div. Polym. Chem.* **1979**, *20* (2), 60.
(2) Michailov, L.; Zugenmaier, P.; Cantow, H.-J. *Polymer* **1968**, *9*, 325.
(3) Seeger, M.; Barrall, E. M., II. *J. Polym. Sci., Polym. Chem. Ed.* **1975**, *13*, 1515.
(4) Ahlstrom, D. H.; Liebman, S. A. *J. Polym. Sci., Polym. Chem. Ed.* **1976**, *14*, 2479.
(5) Mlejnek, O. *J. Chromatogr.* **1980**, *191*, 181.
(6) Sugimura, Y.; Tsuge, S. *Macromolecules* **1979**, *12*, 512.
(7) Tsuge, S.; Sugimura, Y.; Nagaya, T. *J. Anal. Appl. Pyrolysis* **1980**, *1*, 221.
(8) Sugimura, Y.; Usami, T.; Nagaya, T.; Tsuge, S. *Macromolecules* **1981**, *14*, 1787.
(9) Liebman, S. A.; Ahlstrom, D. H.; Starnes, W. H., Jr.; Schilling, F. C. *J. Macromol. Sci., Chem.* **1982**, *A17*, 935.
(10) Haney, M. A.; Johnston, D. W.; Clampitt, B. H. *Macromolecules* **1983**, *16*, 1775.
(11) Randall, J. C. *J. Polym. Sci., Polym. Phys. Ed.* **1973**, *11*, 275.
(12) Bovey, F. A.; Schilling, F. C.; McCrackin, F. L.; Wagner, H. L. *Macromolecules* **1976**, *9*, 76.
(13) Randall, J. C. *J. Appl. Polym. Sci.* **1978**, *22*, 585.
(14) Axelson, D. E.; Levy, G. C.; Mandelkern, L. *Macromolecules* **1979**, *12*, 41.
(15) Usami, T.; Takayama, S. *Macromolecules* **1984**, *17*, 1756.
(16) Shirayama, K.; Okada, T.; Kita, S. *J. Polym. Sci., Part A* **1965**, *3*, 907.
(17) Shirayama, K.; Kita, S.; Watabe, H. *Makromol. Chem.* **1972**, *151*, 97.
(18) Shirayama, K. "Characterization and Physical Properties of Polymers"; Nagasawa, M., Fujita, H., Yamashita, Y., Eds.; Kagakudojin: Kyoto, Kagakuzokan, 1970; Vol. 43, p 131.
(19) Willbourn, A. H. *J. Polym. Sci.* **1959**, *34*, 569.
(20) Mattice, W. L.; Stehling, F. C. *Macromolecules* **1981**, *14*, 1479.
(21) Mattice, W. L. *Macromolecules* **1983**, *16*, 487.
(22) Cudby, M. E. A.; Bunn, A. *Polymer* **1976**, *17*, 345.
(23) Bowmer, T. N.; O'Donnell, J. H. *Polymer* **1977**, *18*, 1032.
(24) Nishioka, A.; Mukai, Y.; Ohuchi, M.; Imanari, M. *Bunseki Kagaku* **1980**, *29*, 774.
(25) Spanswick, J.; Knox, J. R.; Serres, C. *Macromolecules* **1981**, *14*, 1323.

Magic Angle Spinning Carbon-13 NMR Spectroscopy of Three Crystalline Forms of Isotactic Poly(1-butene)

Laurence A. Belfiore,[†] Frederic C. Schilling,[*] Alan E. Tonelli, Andrew J. Lovinger, and Frank A. Bovey

AT&T Bell Laboratories, Murray Hill, New Jersey 07974. *Received March 8, 1984*

ABSTRACT: The same influences which determine the dependence of carbon-13 chemical shifts on chain microstructure in solution spectra appear to be operative also in the solid state. We have investigated the magic angle spinning (MAS) ^{13}C spectra of three forms of isotactic poly(1-butene). Each crystalline form is identified by X-ray diffraction. The percent crystallinity for each sample is determined from density measurements and from the comparison of the melting endotherm with the heat of fusion obtained by differential scanning calorimetry (DSC). Like most isotactic polymers, poly(1-butene) adopts a 3_1 ...(gt)(gt)(gt)... helical conformation, termed form I, at room temperature. This has main-chain dihedral angles of 60° for gauche and 180° for trans conformations. But at ca. 90 °C and above, it prefers an 11_3 helix with g and t angles of 77° and 163°, respectively, called form II. When prepared in film form by solvent (chloroform) evaporation, it yields form III, a 4_1 helix with g and t angles of 83° and 159°. Form I gives a well-resolved MAS spectrum. The resonances of form II are much broader and somewhat deshielded compared to those of form I. The spectrum of form III is well resolved, with all resonances markedly deshielded compared to those of form I. (There is also a splitting of the methyl resonance, attributed to crystal packing effects.) This deshielding can be consistently interpreted on the hypothesis that the γ-gauche shielding parameter, normally ca. −5 ppm when the gauche angle is ca. 60°, is angle dependent, decreasing to ca. −2.5 ppm at 81–83° and to an intermediate value at 77°.

Introduction

The same influences which determine the dependence of carbon-13 chemical shifts on chain microstructure in the solution NMR spectra of macromolecules appear to be operative also in the solid state. Thus, the solid-state magic angle spinning (MAS) carbon-13 spectra of crystalline isotactic[1-4] and syndiotactic[4] polypropylenes may be convincingly interpreted in terms of γ-gauche interactions with the same γ-gauche shielding parameter of ca. −5 ppm used in the prediction of the solution carbon-13 spectrum of atactic polypropylene.[5] In addition, the differences in chemical shift observed between crystalline and amorphous carbons in polyethylene,[6] poly(oxymethylene),[7] and poly(oxyethylene)[8] can also be explained on the basis of γ-gauche interactions.[9] This difference in chemical shift is the result of different conformations adopted by crystalline and amorphous chains.

Like most isotactic vinyl polymers, isotactic poly(1-butene) adopts a 3_1 ...(gt)(gt)(gt)... helical crystalline conformation at room temperature.[10] The chains have dihedral angles of 60° for gauche and 180° for trans conformations and are packed in a trigonal unit cell (form I). But at ca. 90 °C and above this polymer is known to prefer a tetragonal form, called form II, in which the chain conformation is an 11_3 helix with alternating "gauche" and "trans" angles of 77° and 163°, respectively.[11-13] At room temperature form II spontaneously transforms into form I within a few days. In films, this transformation proceeds from the surface inward[14] and is in general associated with pressure and mechanical stress. We have found that in bulk it is markedly accelerated by magic angle spinning (cf. seq.). There is also a third polymorph, form III,[15-18]

[†] Present address: Colorado State University, Fort Collins, CO 80523.

0024-9297/84/2217-2561$01.50/0